

Nuclear import of Cdc13 limits chromosomal capping

Sofiane Y. Mersaoui, Erin Bonnell and Raymund J. Wellinger*

Department of Microbiology and Infectiology, Faculty of Medicine and Health Sciences, Université de Sherbrooke, 3201 Rue Jean Mignault, Sherbrooke, QC J1E 4K8, Canada

Received October 13, 2017; Revised January 18, 2018; Editorial Decision January 27, 2018; Accepted January 30, 2018

ABSTRACT

Cdc13 is an essential protein involved in telomere maintenance and chromosome capping. Individual domain analyses on Cdc13 suggest the presence of four distinct OB-fold domains and one recruitment domain. However, it remained unclear how these subdomains function in the context of the whole protein *in vivo*. Here, we use individual single domain deletions to address their roles in telomere capping. We find that the OB2 domain contains a nuclear localization signal that is essential for nuclear import of Cdc13 and therefore is required for chromosome capping. The karyopherin Msn5 is important for nuclear localization, and retention of Cdc13 in the nucleus also requires its binding to telomeres. Moreover, Cdc13 homodimerization occurs even if the protein is not bound to DNA and is in the cytoplasm. Hence, Cdc13 abundance in the nucleus and, in consequence, its capping function is strongly affected by nucleo-cytoplasmic transport as well as nuclear retention by DNA binding.

INTRODUCTION

Functional telomeres, the terminal parts of linear chromosomes, are essential for safeguarding the genome. Their structure and organization are highly conserved amongst eukaryotic species. For example, telomeric DNA consists of short, repeated G-rich sequences generally ending with an extended overhang of the 3'-end (1,2). A certain minimal number of the species specific repeats is essential for telomere function as it is required for the binding of specialized telomeric proteins (1–3). The assembled functional telomeric complex protects ends from inappropriate resection, thus preventing DNA damage checkpoint activation and/or chromosome end to end fusions (1,2). A second function of telomeres is that of counteracting the progressive losses of terminal DNA that occurs during each round of replication due to the end-replication problem (4). Indeed, short telomeres are elongated by a specialized and conserved reverse transcriptase called telomerase (5,6). In

budding yeast, both telomere elongation and the telomere capping function are orchestrated by a heterotrimeric complex composed of the essential proteins Cdc13, Stn1 and Ten1, respectively (abbreviated as CST; (1,7–9)). CST complexes with similar functions exist in plants, fission yeast and mammals where they are associated with limiting telomerase-mediated telomere lengthening, lagging strand synthesis on telomeres and rescuing a stressed replication fork during replication of difficult sequences (10–16). There may be an analogous complex in the fruit fly (17,18), pointing to deeply rooted conserved features of chromosome capping mechanisms. In humans, mutations in either hCTC1 or hSTN1 have been shown to cause Coats Plus syndrome, characterized by telomere dysfunction not necessarily associated with short telomeres (13,19).

Molecular modeling and direct structure function experiments on the budding yeast CST proteins revealed similarities with the heterotrimeric replication protein A (RPA) (20–22). Within CST, Cdc13 is thought to be the major hub for the various CST functions and it in particular determines DNA binding activity *in vitro* and *in vivo* (23–26). Loss of Cdc13 elicits a Rad9-dependent cell cycle arrest (9) and particularly the temperature-sensitive *cdc13-1^{ts}* allele has been used extensively to study general DNA damage checkpoint function and cell cycle arrest mechanisms. However, the molecular details of why telomeres appear completely uncapped in *cdc13-1* cells incubated at restrictive temperatures remained unknown.

Studies on biochemical properties, including crystallization, of individual fragments revealed that Cdc13 may be composed of four distinct Oligosaccharide/oligonucleotide Binding (OB)-fold domains named OB1, OB2, OB3 (the DNA Binding Domain) and OB4, in addition to a recruitment domain (RD) that is in between OB1 and OB2 (Figure 1A; (21–24,27–32)). The N-terminal OB1 is proposed to mediate Cdc13 homodimerization (21). However, preventing this dimerization has little effect on capping and only slightly affects telomere homeostasis (21,29). A portion of Cdc13-OB1 also serves to anchor DNA Polymerase α -primase to the telomere to achieve C-strand synthesis (21,31,33,34). The RD domain just downstream of OB1 interacts with the telomerase subunit Est1, thereby mediating the link between telomerase and telomeres (25,35). Mu-

*To whom correspondence should be addressed. Tel: +1 819 821 8000 (Ext. 75214); Email: Raymund.Wellinger@usherbrooke.ca
Present address: Sofiane Y. Mersaoui, Lady Davis Institute for Medical Research, Departments of Oncology and Medicine, McGill University, Montreal, Canada.

the nuclear localization of the mutated protein, suppresses the growth arrest phenotype of *cdc13-1* cells at restrictive temperature and ensures functional telomere capping and cell viability on its own. In addition, nuclear retention of the Cdc13 protein also requires its ability to interact with DNA. Our data further argue that inside cells, Cdc13 occurs as a constitutive dimer, even if not bound to DNA. Thus, neither the *cdc13-1* mutation, OB2 deletion, nor the loss of telomeric DNA interaction affected homodimer formation *in vivo*. Our results therefore for the first time explain an extensive literature on the phenotypes of the *cdc13-1* mutation. In addition, we note that for the human CTC1 protein, which is part of hCST, cytoplasmic mislocalization is a feature of a number of mutations that are associated with Coats Plus syndrome (42).

MATERIALS AND METHODS

Plasmid constructions

All plasmids are listed in Supplementary Table S1 and are derived from the original pVL438 (*CEN*, *URA3*, *CDC13* (35)). All described mutations were achieved by PCR mutagenesis (primer sequences are supplied upon request) and verified by sequencing. All strains used in this study are listed in Supplementary Table S2. Note that all strains are annotated for where they were used in the experiments/figures.

Southern blot and in-gel hybridization analysis

DNA was extracted from saturated liquid cultures using a glass bead procedure (43). For native in-gel analyses, DNA was extracted from mid-log phase cultures. The DNA was digested with XhoI, fragments separated on agarose gels and the gels hybridized without any denaturation using a CA oligonucleotide probe as described in (44). For loading controls, after imaging of the signals from the native DNA gels, the DNA in the gels was denatured and gels re-probed with the CA oligonucleotide. For quantification, whole-lane signals from native hybridization were normalized first to the signal obtained from denatured, total DNA, and then compared to the control strains, as in (44). Experiments were done at least three times.

Chromatin Immuno-Precipitation (ChIP) analysis

ChIP was performed as described in (45,46) and the methodology is extensively detailed in the Supplemental Methods section. Briefly, strains were grown to OD = 1 and fixed with 1% (v/v) formaldehyde for 5 min. Cells were suspended in ChIP-lysis buffer containing PMSF. Flash frozen 'Popcorn' was obtained by dropping cells into liquid nitrogen and cell lysis was achieved in liquid nitrogen using a freezer mill method. After melting, samples were supplemented with a protease inhibitor cocktail and subjected to sonication. Soluble fractions were subjected to immunoprecipitation with Pierce™ Protein A/G magnetic beads using 2 µg of mouse monoclonal anti-Myc antibody for 2 h at 4°C. ChIP-beads were washed and crosslinks reversed overnight at 65°C. Samples were subjected to RNase (1 h

and Proteinase K (6 h) incubation. Then, DNA was extracted by a phenol/chloroform and purified by a Qiagen PCR kit purification. Immunoprecipitates and Input DNA were analyzed by qPCR (see Supplemental Methods for details).

Co-immunoprecipitation (Co-IP) and Western blot (WB)

Protein extracts for WB were prepared using a trichloroacetic acid method. Proteins were separated by 6% SDS-PAGE for Cdc13-Myc blots and 10% for Rad53 blots as described in (40). Blotting was performed using indicated antibodies. Signals were revealed using horseradish peroxidase-conjugated secondary antibody with the enhanced chemiluminescence detection kit. CoIP was prepared as previously described (47). Cells from 0.5 OD cultures were pelleted and resuspended within appropriate lysis buffer supplied with protease inhibitors and PMSF. Flash frozen 'Popcorn' were made as above and ground in a Freezer/Mill. The powder was thawed on ice and cleared by centrifugation. Equivalents of 5 mg protein in the soluble fraction were adjusted for Co-IP in 1 ml of total volume. 20 µg of anti-Myc antibody were added and extracts incubated for 2 h at 4°C. IP was performed with 30 µl of a slurry with magnetic beads (Pierce™ Protein A/G) for another 2 h. For the HA IP experiments, 1 ml extract was added to 30 µl of a suspension of magnetic beads coated with anti-HA antibody. Beads were then removed and washed with TMG Lysis buffer. If indicated, beads were incubated with DNase I for 1 h at 37°C.

Immunofluorescence and microscopy

Cell cultures at OD 0.5 were fixed with 5% formaldehyde and suspended in 1 ml of lysis buffer for cell wall digestion (see Supplemental Methods for details). Cells were then resuspended and dropped onto immunofluorescence glass with a polylysine treated surface. After methanol fixation and acetone treatment, cells were air dried and treated with a PBS solution containing BSA and supplemented with a mix of primary antibody (anti-Myc and anti-tubulin or anti-PGK) for 2 h. Secondary antibodies (Alexa) conjugated to specific fluorophores were added in PBS buffer with BSA (1 mg/ml) for 2 h. After several washes, DNA was stained with DAPI and mounted on cover-slips. Pictures were acquired with a Zeiss mRm Axiocam mounted on an axio observer Z1 inverse microscope using Zen 2012 software as in (47). Localization and co-localization was determined manually. Signal intensity for ratio determinations was analyzed by Columbus software. Statistical *t*-test analyses are provided from at least three independent experiments.

RESULTS

Cdc13 OB2 and OB3 are essential for viability, while the RD and OB4 are essential for telomere length control

In order to better understand the role of each domain in Cdc13, we generated a Myc tagged version expressed from a low copy plasmid (*CEN/ARS*) and in which each domain

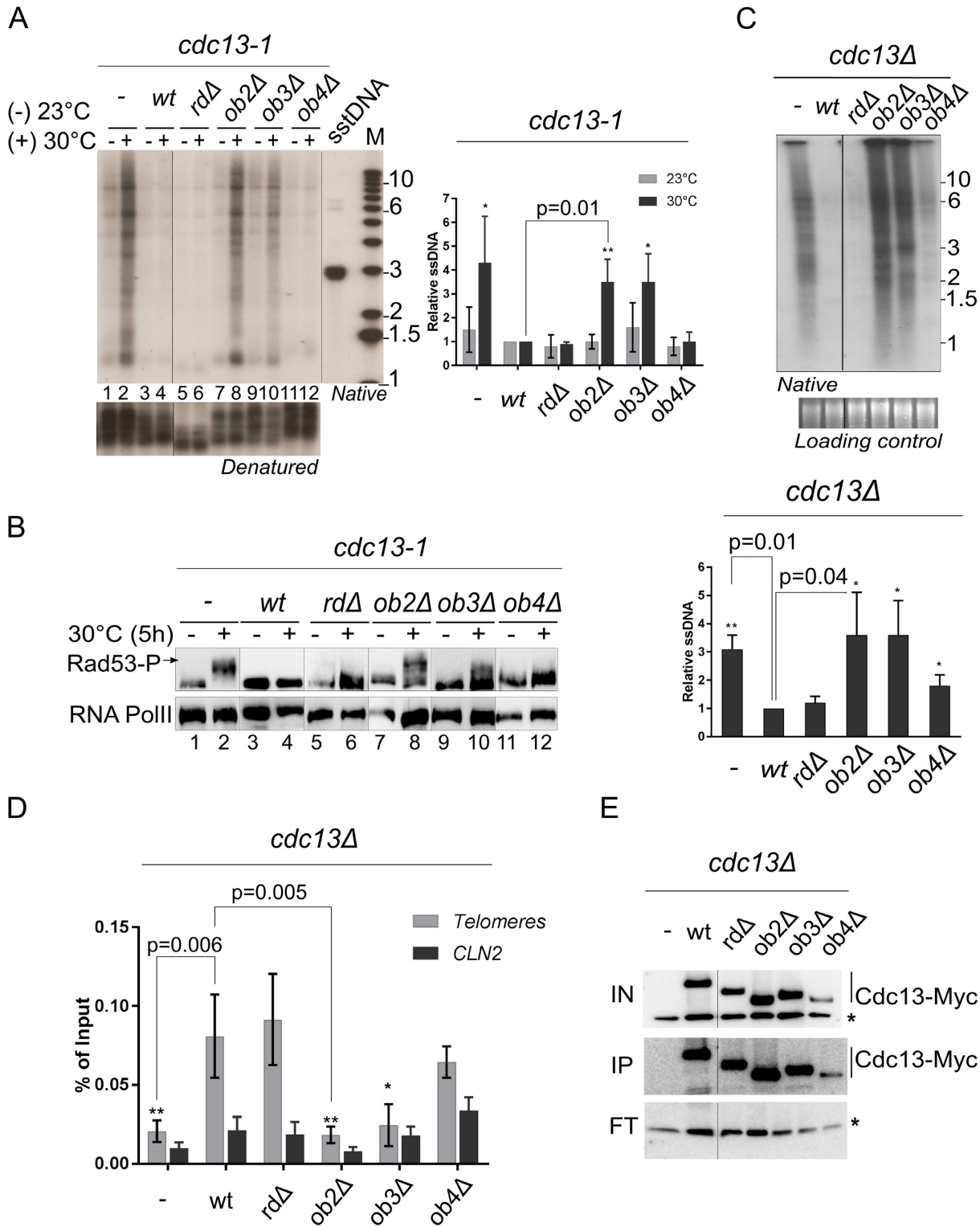


Figure 2. Cdc13-ob2Δ and Cdc13-ob3Δ proteins lack DNA interaction and cause a loss of capping. (A) Native in-gel hybridization of DNA derived from *cdc13-1* strains expressing indicated alleles of *CDC13* incubated at permissive and restrictive conditions for 2 h. (–) Growth at 23°C; (+) growth at 30°C. sstDNA is a single stranded control DNA. Bottom panel: same gel re-hybridized after denaturation to control for DNA loading. Panel to the right: relative ssDNA signal detection, wt signal is set as 1. (B) Western blot for hyper phosphorylation status of Rad53 in each strain as indicated in (A); (–) growth at 23°C; (+) incubated at 30°C for 5 h. RNA PolIII is the loading control. (C) Upper panel: Native In-gel hybridization of an adapted *cdc13Δ* strain expressing the indicated mutated Cdc13 proteins. Middle panel: EtBr stain as loading control. Lower panel: relative quantification ssDNA as in (A) (**P* < 0.05, and ***P* < 0.01 obtained by *t*-test for A and C). (D) ChIP of indicated Myc-tagged Cdc13 proteins expressed in the adapted *cdc13Δ* strain. Relative quantification as % of input for the indicated strains. Black boxes: values for telomeric sequence enrichment; Gray box: values for an unrelated locus (*CLN2*) as negative control. (–) Indicates untagged version of Cdc13. (E) Western blot of IP Cdc13-Myc variants in used in (D). * Non-specific signal.

was deleted individually (see Figure 1A for details). Deleting the N-terminal OB1 caused a dramatic destabilization of the protein and causes a null phenotype (Figure 1B and Supplementary Figure S1D). However, that characteristic is not informative and OB1 deletions will not be discussed further. The remaining four alleles were first tested for their ability to complement a *cdc13* Δ allele in haploid spores. In line with previous results, two of the four new *CDC13* alleles, *cdc13-rd* Δ and *cdc13-ob4* Δ , are not immediately essential for Cdc13-function (Supplementary Figure S1A). After further outgrowth, cultures of cells containing the *cdc13-rd* Δ allele displayed classical signs of senescence, similar in phenotype to *tlc1* Δ cells lacking telomerase altogether (Supplementary Figure S1B). Moreover, both *cdc13-rd* Δ and *cdc13-ob4* Δ complemented the temperature defect of the *cdc13-1* strain at all temperatures tested (Figure 1C and Supplementary Figure S1C). In contrast, the *cdc13-ob2* Δ and *cdc13-ob3* Δ alleles could not complement an absence of Cdc13 and therefore, the two OB2 and OB3 domains are essential for Cdc13 function and cell viability (Supplementary Figure S1A). Transforming *Cdc13-ob2* Δ or *Cdc13-ob3* Δ separately into a strain that contains the hypomorphic *cdc13-1* allele also did not suppress the thermosensitivity of this strain (Figure 1C). This lack of complementation is not due to protein expression levels: western blot analysis on total protein extracts showed that the expression level of the mutant proteins is comparable to the wildtype (Figure 1B). Southern blot analyses of telomeric restriction fragments using DNA derived from cells that harbor the *cdc13-1* allele and the indicated deletion allele were performed after 120 generations of growth (Figure 1D). Cells with the *Cdc13-ob2* Δ or the *Cdc13-ob3* Δ protein do not grow at 30°C while when grown at permissive temperature, telomeres were of normal length (Figure 1D). As expected, cells expressing the *Cdc13-rd* Δ protein and grown at 30°C contained extremely short telomeres (Figure 1D). Remarkably however, the senescence phenotype and survivor formation was somewhat delayed from normally 100 generations to ~220 generations in this situation (Supplementary Figure S1F). These results suggest that the *cdc13-1* allele can partially trans-complement an allele that lacks the recruitment domain (*cdc13-rd* Δ), even if cells are grown at restrictive temperature.

In the complete absence of telomerase, for example if cells lack the RNA component, a small subset of them will switch to a recombination-based telomere maintenance and such cells are called survivors. They show at least two distinct phenotypes in terms telomeric restriction fragments: type I cells display an amplification of telomere associated sequences and very short terminal repeat tracts, whereas type II cells display many bands of highly variable distinct sizes (for this latter, see Supplementary Figure S1E, lane 1) (1,48). In *Cdc13*-independent cells, also called adapted *cdc13* Δ cells that were derived from type-II survivors (41), the signals for telomeric restriction fragments are extremely smeary and almost lacking distinct bands (see example in Supplementary Figure S1E, lane 2). However, this phenotype reverts to the survivor pattern after reintroduction of a wt Cdc13 protein (Supplementary Figure S1E, lane 3; (41)). The *Cdc13-rd* Δ and *Cdc13-ob4* Δ proteins were sufficient to also revert this phenotype back to distinct bands (Supple-

mentary Figure S1E, lanes 4, 7). However, introduction of the *Cdc13-ob2* Δ or *Cdc13-ob3* Δ proteins did not yield such a phenotype reversion, suggesting that these alleles caused a total loss of all functions (see lanes 5 and 6, Supplementary Figure S1E). As previously observed with the *cdc13-2* allele that is located in the RD domain, the results with the *Cdc13-rd* Δ protein confirm that this domain does not contribute to the capping function (25), and by extension this also applies to the OB4 domain. Given that DNA binding is thought to be required for all functions of Cdc13, the deletion of OB3 (DBD) was expected to yield the complete loss of function phenotypes observed here. However, the fact that OB2 was equally essential was unexpected.

Both OB2 and OB3 are required for DNA binding *in vivo*

To better understand the role of the OB2 domain, we analyzed the functionality of the *Cdc13-ob2* Δ protein in telomere capping in more detail. One of the hallmarks of loss of Cdc13-mediated capping is extensive 5'-strand resection from the telomeres that can be detected via a native DNA in-gel hybridization assay (44). For the analyses here, *cdc13-1* cells also expressing the indicated domain-deleted alleles were incubated at permissive temperature (– in Figure 2A) or shifted to 30°C, the restrictive temperature for *cdc13-1*, for 2h (+ in Figure 2A). Without any plasmid encoded version of Cdc13, 5' resection and the accumulating ssDNA is readily detectable (Figure 2A, compare lane 2 to lane 4). The *Cdc13-rd* Δ and *Cdc13-ob4* Δ can fully complement this capping defect, as no increase in ssDNA signal is detectable as if a wt Cdc13 was expressed (Figure 2A, lanes 4, 6 and 12). However, on DNA derived from cells expressing the *Cdc13-ob2* Δ and *Cdc13-ob3* Δ proteins, a strong capping defect is detected (Figure 2A, lanes 8 and 10). This ssDNA accumulation results in Rad53 hyperphosphorylation which is indicative of an activation of the DNA damage checkpoint (Figure 2B lanes 2, 8 and 10; Supplementary Figure S2A). In order to address the possibility of a partial trans-complementation that could interfere with interpretations, the above experiment was performed in two additional ways. In the first, the endogenous Cdc13 is induced to be degraded via the degron system and therefore removed (49). Consistent with the results with the situation with the *cdc13-1* allele above, expressing the Wt protein or the *Cdc13-rd* Δ or *Cdc13-ob4* Δ proteins fully protected the telomeres from resection (Supplementary Figure S2B). In contrast, expression of *Cdc13-ob2* Δ or *Cdc13-ob3* Δ revealed a strong capping defect and checkpoint activation after 3 h of degron induction (Supplementary Figure S2B–D). In the second situation, we performed the same analyses in an adapted *cdc13* Δ strain. Again as above, the *Cdc13-rd* Δ and the *Cdc13-ob4* Δ conserved the capping capacity and virtually no ssDNA accumulation was detected (Figure 2C), while the *Cdc13-ob2* Δ and *Cdc13-ob3* Δ expressing cells show a strong capping defect (Figure 2C). Hence, in all situations tested, cells expressing the *Cdc13-ob2* Δ protein behave like those expressing the *Cdc13-ob3* Δ , which cannot bind DNA. Therefore we assessed whether the *Cdc13-ob2* Δ can be associated with DNA *in vivo* by ChIP assays using cells that expressed the generated alleles in either adapted *cdc13* Δ or in *cdc13-1* strains. As expected from previous

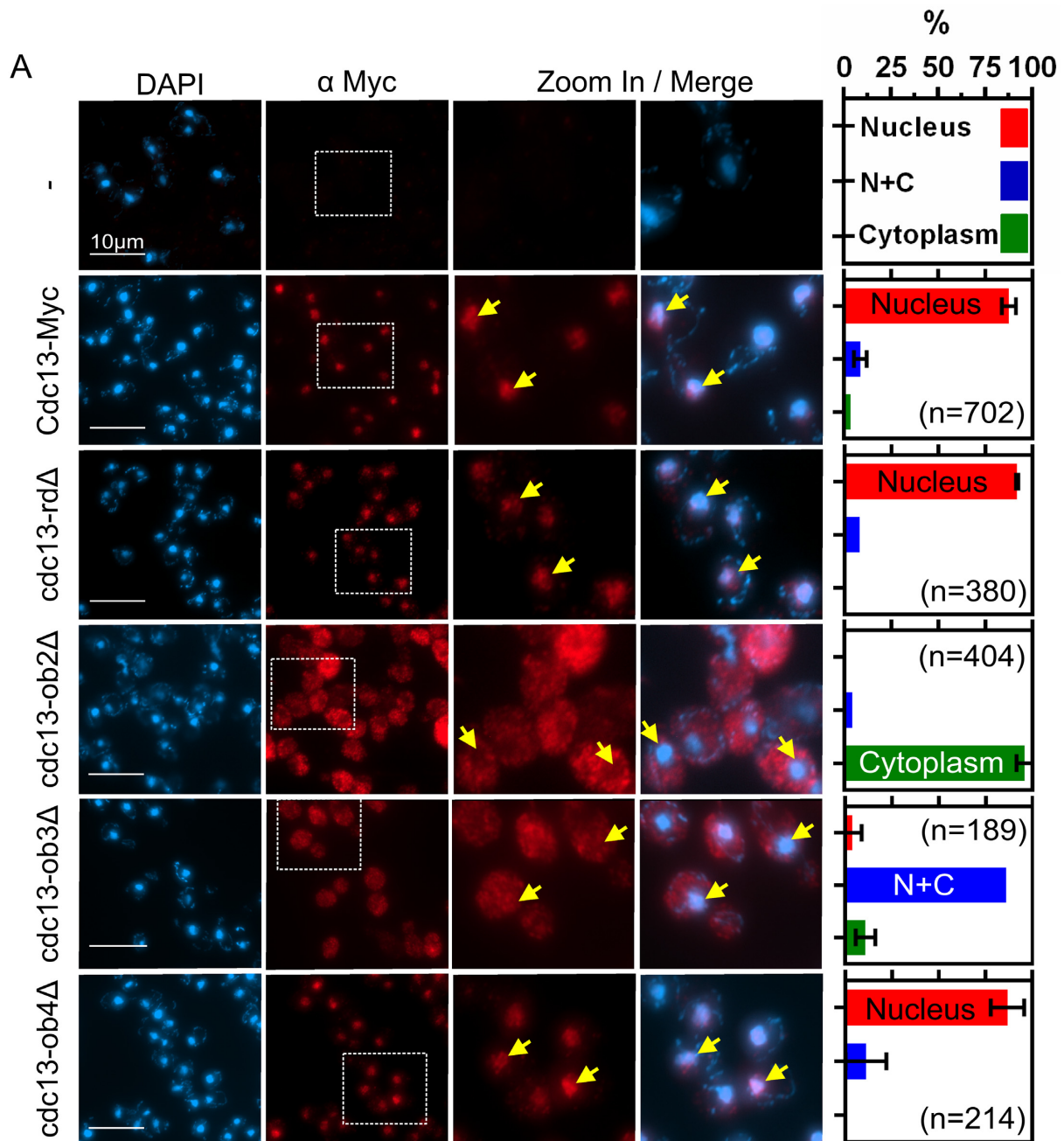


Figure 3. Cdc13-ob2 Δ mislocalizes to the cytoplasm. (A) Immunofluorescence using adapted *cdc13* Δ cells expressing the indicated Myc-tagged Cdc13 proteins. Blue: DAPI coloration, nuclear DNA; Red: Myc-tagged protein. Stippled White square: zoom-in. Graphics on the right represents the distribution of Cdc13-Myc protein in cells (Nucleus, Cytoplasm, N+C = localization in both nucleus and cytoplasm; (n) total number of cells analyzed in at least three independent experiments. Error bars represent \pm SEM. Yellow arrowheads indicate particularly telling cells. (B) Graphic outline of the predicted cNLS localization in the Cdc13 protein as analyzed by cNLS Mapper (50). *P* value indicates the confidence level as calculated by NLS Mapper.

data, both the Cdc13-rd Δ and Cdc13-ob4 Δ proteins still bind DNA *in vivo* (Figure 2D and Supplementary Figure S2E) (24,25). In contrast, the Cdc13-ob2 Δ protein behaved indistinguishably from the Cdc13-ob3 Δ protein, suggesting that it does not associate with ssDNA *in vivo* (Figure 2D and Supplementary Figure S2E). Western blots after IP immunoprecipitation confirmed that the mutated proteins could be enriched equally with the anti-myc antibody (Figure 2E). In conclusion, the Cdc13-ob2 Δ protein appeared not to be associated with DNA *in vivo* despite the fact that it contained the complete OB3 domain that was thought to be sufficient for all DNA binding activity of Cdc13 (28) and that the OB2 alone did not associate with DNA *in vitro* (24,29)

The OB2 domain is required for nuclear localization of Cdc13

The above results suggested either a general misfolding with complete loss of function for the Cdc13-ob2 Δ protein or a mislocalisation. In order to assess the latter hypothesis, we used the adapted *cdc13* Δ strains that grow even in the complete absence of Cdc13 and in which we localized tagged mutated proteins by immuno-fluorescence. When these cells express the wild type Cdc13-Myc protein, telomeres are capped (Figure 2C) and anti-myc staining revealed discrete staining almost exclusively in the nucleus, as expected (Figure 3A, second row). Quantification of signal intensities for Cdc13-Myc (red) versus DNA (blue) showed that more than 75% of the signal co-localized (Figure 3A, right, Supplementary Figure S3). The Cdc13-rd Δ and Cdc13-ob4 Δ proteins were also found to localize to the nucleus (Figure 3A, Supplementary Figure S3), in line with the functional capping data above. In contrast, the Cdc13-ob2 Δ and Cdc13-ob3 Δ proteins showed differing and distinct phenotypes. The Cdc13-ob3 Δ protein displayed a non-specific localization pattern: it is found equally abundant in the cytoplasm and nucleus (Figure 3A). Remarkably, the Cdc13-ob2 Δ protein appears absent from the nucleus and localized almost exclusively to the cytoplasm (Figure 3A, Supplementary Figure S3B). This cytoplasmic localization suggested that the OB2 domain determines nuclear localization via import and/or the introduced mutations induced an export via a normally hidden nuclear export signal. Computational analyses of the Cdc13 protein actually predict a bipartite nuclear localization signal (NLS)(Figure 3B, (50)). In fact, this predicted NLS localizes on the N-terminal side of OB2 (a.a. 325–350). Indeed, while deleting a.a. 289–328 is well tolerated and results in a functional protein, deleting a.a. 329–368 results in a complete loss of function (Supplementary Figure S4A and B). If OB2 determined nuclear import of Cdc13, introduction of a strong exogenous nuclear localization signal into the Cdc13-ob2 Δ protein should restore at least some functionality. Indeed, when we introduced the SV40 NLS between the RD domain and the OB3 of the Cdc13-ob2 Δ , a construct called Cdc13-ob2 Δ -NLS, >70% of the nuclear signal was restored (Figure 4A). As a control, we also added an NLS sequence in place of the OB3 between the OB2 and the OB4 and obtained a similar result (Figure 4A; Supplementary Figure S5A). Western blots confirmed that these proteins were expressed normally, even if the Cdc13-ob2 Δ -NLS protein appears slightly

less abundant (Supplementary Figure S4C). Nevertheless, the rescued localization of the Cdc13-ob2 Δ -NLS protein to the nucleus is sufficient to allow *cdc13-1* cells to grow at 30°C (Figure 4B) and prevent the generation of ssDNA by 5'-end resection (Figure 4C). Expression of this protein also abrogates Rad53 phosphorylation after incubation at 30°C (Figure 4D), but Rad53 still can be induced by incubation of the same strain with the radiomimetic Bleomycin, which induces DNA damage in a locus non-specific fashion (Supplementary Figure S4D). Consistent with these results obtained with *cdc13-1* cells, the telomere capping function was also restored in the adapted *cdc13* Δ cells (Supplementary Figure S4E). These rescue phenotypes can be ascribed specifically to the introduced NLS signal peptide, because if this peptide contains an abrogating mutation (nlsm), all the complementing phenotypes were lost (Figure 4B and Supplementary Figure S4E). When the Cdc13-ob2 Δ -NLS protein is expressed from a multicopy plasmid as the sole allele expressed, it actually allows cell growth (Figure 4E). Finally, telomeres in these cells harboring the Cdc13-ob2 Δ -NLS multicopy plasmid had lengthened significantly beyond wt (Figure 4F). These findings strongly suggest that the N-terminal part of the OB2 domain is involved in nuclear import of the Cdc13 protein. In contrast to the results with the Cdc13-ob2 Δ -NLS protein, the Cdc13-ob3 Δ -NLS protein could not rescue the capping defect in adapted *cdc13* Δ cells (Supplementary Figure S4E), even though it was expressed at a level similar to wt (Supplementary Figure S4C) and properly localized to the nucleus (Figure 4A, Supplementary Figure S5A). These data corroborate the fact that the OB3 is required for DNA binding and hence all functions of Cdc13.

Given these dramatic mis-localization findings with the Cdc13-ob2 Δ protein, we wondered whether a similar effect could explain the phenotypes of the Cdc13-1 protein as well. The a.a. change in this mutation is in OB2 and we thus performed immuno-fluorescence studies with a Myc-tagged Cdc13-1 at different incubation temperatures (Figure 5). While the nuclear localization of the wt Cdc13 is not affected by temperature, there is a stark difference in the localization of the Cdc13-1-Myc protein between cells incubated at 23°C versus 35°C (Figure 5A and B, Supplementary Figure S5B). The predominantly nuclear staining of the Cdc13-1-Myc protein at 23°C is by and large lost for a very diffuse cytoplasmic staining at 35°C. This final phenotype is comparable to that displayed by the Cdc13-ob2 Δ protein (see Figure 3A). Cells expressing the Cdc13-1-Myc protein and which are incubated at the restrictive temperature do induce Rad53 phosphorylation (Figure 5C) and arrest with a G2/M morphology, as expected. Moreover, in adapted *cdc13* Δ cells expressing the Cdc13-ob2 Δ protein, the protein appears always in the cytoplasm, irrespective of the specific cell cycle phase of the analyzed cell (Figure 3A).

A previous investigation on the reasons for the temperature-sensitivity of the *cdc13-1* allele showed that an absence of the karyopherin beta Msn5 aggravated it (51). Given our results, we examined the localization of Cdc13-1 in *msn5* Δ cells at 23°C. As mentioned above, the cytoplasmic localization of Myc-tagged Cdc13-1 at this temperature is subtle, but noticeable, in MSN5^{wt} cells. This phenotype becomes very much aggravated in *msn5* Δ cells,

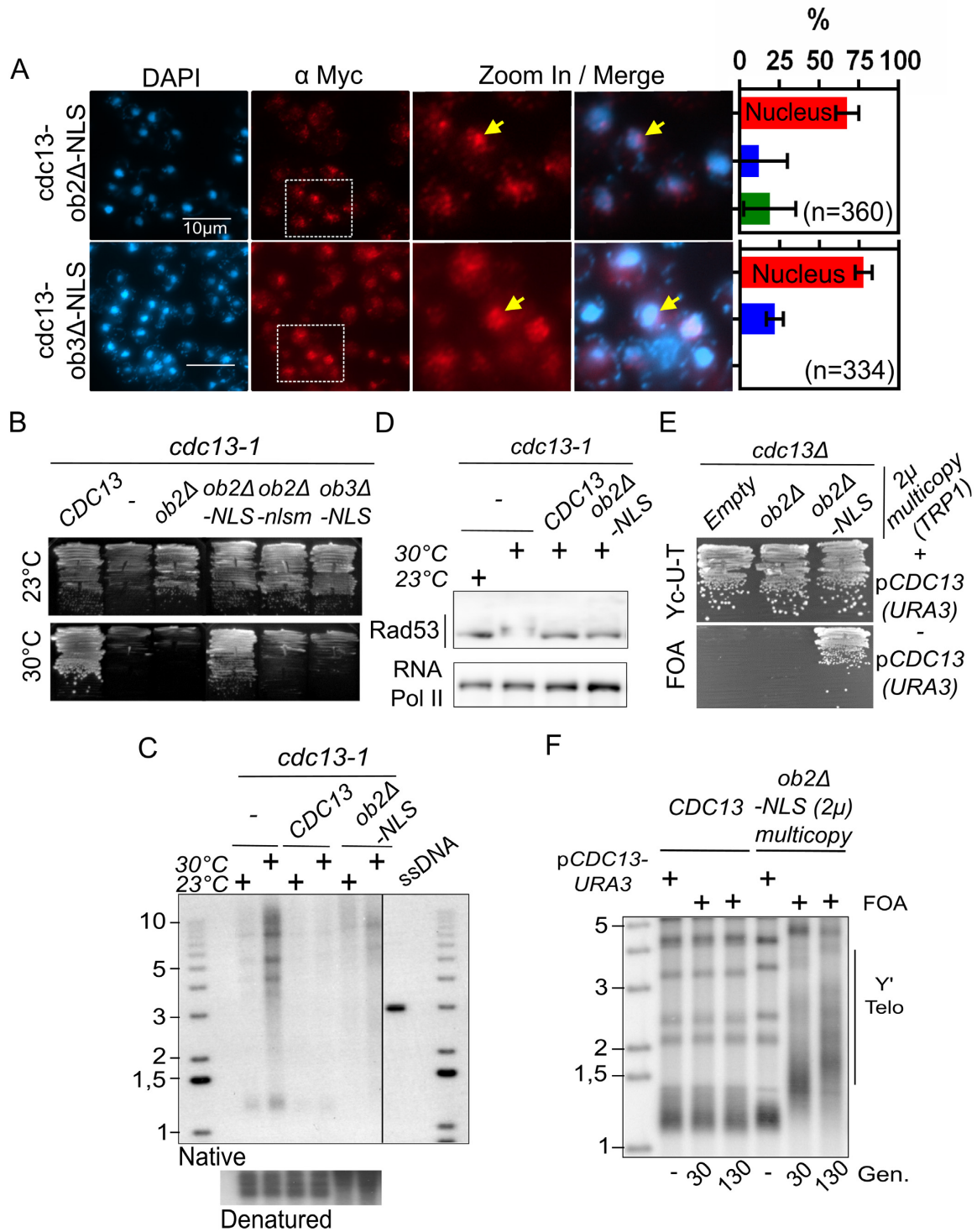


Figure 4. Phenotype reversions after adding an NLS to Cdc13-ob2Δ. (A) Immunofluorescence of Myc-tagged Cdc13-ob2Δ-NLS and Cdc13-ob3Δ-NLS proteins in the adapted *cdc13Δ* strain as in Figure 3A. (B) Complementation of growth in the *cdc13-1* at 30°C. The Cdc13-ob2Δ-nlsm protein harbors a mutated non-functional NLS. (C) In-gel hybridization analysis of telomeric DNA from the indicated strains. (D) Western blot for Rad53 phosphorylation in proteins derived from strains as in (C) grown at 23°C or 30°C as indicated. (E) Expression of the Cdc13-ob2Δ-NLS protein from a 2μ plasmid yields viable cells. Cells before FOA selection do contain a wtCdc13 gene on a URA3-plasmid (top row Yc-U-T; + *pCDC13* (*URA3*)). After selection on FOA plates, cells contained *TRP1* plasmids with the indicated *CDC13* allele (empty = pRS424, no Cdc13; *ob2Δ* = pRS424+Cdc13-ob2Δ; *ob2Δ-NLS* = pRS424+Cdc13-ob2Δ-NLS; as indicated on top). (F) Telomere southern blot analysis of DNA from cells derived from panel (E). Cells before FOA selection do contain a wtCdc13 gene on a URA3-plasmid (lanes indicated with a - below gel); after FOA selection, cells contained the indicated allele (wtCdc13 or Cdc13-ob2Δ-NLS; as indicated on top of gel) and were grown for 30 or 130 generations (indicated below gel).

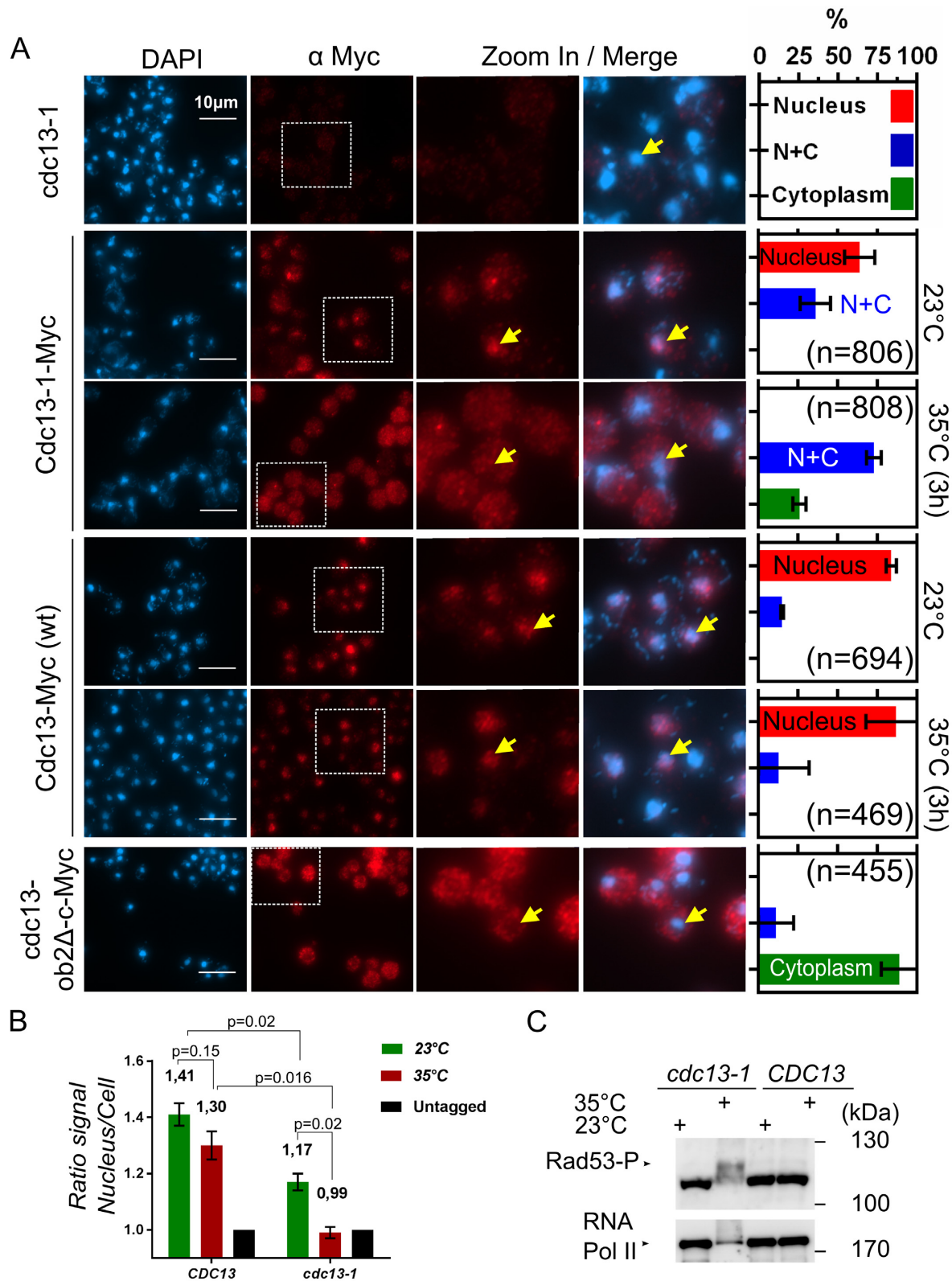


Figure 5. The *cdc13-1* mutation causes mislocalization. (A) Immunofluorescence on strains expressing the Cdc13-Myc, Cdc13-1-Myc or the Cdc13-ob2Δ-c-Myc protein. The *cdc13-ob2Δ-c* lacks a.a. 369–408 (see Supplementary Figure S4A). Analyses are as in Figure 3. Temperatures of experiments are indicated on the right. (n) Total number of cells analyzed. Error bars represent \pm SEM. (B) Quantification of the nuclear signal versus total signal obtained with the anti-Myc antibody in the indicated strains and conditions. Untagged proteins are set as 1. Calculated Mean value is indicated on the top of each bar and error bars represent \pm SEM. Indicated *P*-values (*p*) are provided by *t*-test between the two defined conditions. (C) Western blot for Rad53 phosphorylation of indicated strains as in panel (A).

even at 23°C (Figure 6A, Supplementary Figure S5C). Remarkably, in *msn5Δ* cells, a certain level of cytoplasmic localization can be detected even for the wt Cdc13 protein (Figure 6, second row), suggesting that Msn5 does indeed play a role in the proper localization of Cdc13.

Constitutive Cdc13 dimerization is independent of OB2

Previous results obtained with an isolated OB2 domain protein suggested a role in Cdc13 dimerization which may inhibit Cdc13-Stn1 interactions (29). In order to analyze the effect of an OB2 deletion on potential dimerization in the context of the complete Cdc13 protein, we performed *in vivo* co-immunoprecipitation experiments in a haploid strain that expressed two tagged versions of Cdc13 (13xMyc or 3xHA). When both Cdc13 proteins were wild-type versions, they were expressed at about equal levels and they can be co-immunoprecipitated, as expected (Supplementary Figure S6A–C). This interaction was not dependent on telomeric DNA, as dimerization was detectable even after DNase I treatment of the extracts and the IP fractions did not contain detectable levels of telomeric DNA sequences (Figure 7A). As expected, in this situation no detectable Rap1 protein was in the precipitate (Supplementary Figure S6D). Previous experiments demonstrated that the constitutive G-strand overhang on telomeres in *mre11Δ* cells were extremely short and most likely only a single Cdc13 molecule would fit on it (52). Cells with the *mre11Δ* allele and arrested in G0 for 48 h thus reflect a situation with minimal opportunity for Cdc13 to dimerize on the overhang DNA, yet the two Cdc13 versions still co-precipitated in extracts from these cells (Figure 7B). A previously described *CDC13* allele called *cdc13-4R* contains 4 a.a. changes in OB1 and this allele was reported to have lost the ability to form dimers (21). Indeed, in the co-immunoprecipitation assays used here, dimerization of Cdc13-4R proteins could not be detected (Figure 7C, left panel). These setup experiments thus provided a solid platform with which to verify the interaction potential of the specific domain-deleted alleles. In order to avoid problems related to inviability of cells, for these next experiments we used the adapted *cdc13Δ* strain co-expressing the two differently tagged copies of the same alleles and compared co-immunoprecipitation profiles. Deletion of either the RD, the OB2 or the OB4 domains did not impair dimer formation (Supplementary Figure S6E). Consistent with this result, the hypomorphic *cdc13-1* allele also did not impair the ability of the Cdc13-1 protein to be co-immunoprecipitated, even after 2 h of incubation of the cells at the restrictive temperature (Figure 7D). In contrast, the Cdc13-ob3Δ protein completely lost the ability to form a dimer (Supplementary Figure S6E). Remarkably, the Cdc13-ob3Δ also could not be co-immunoprecipitated with a wt protein (Supplementary Figure S6E, middle right). Given that the tagged Cdc13-ob2Δ protein still can be co-immunoprecipitated, yet mislocalizes to the cytoplasm and is not associated with telomeric DNA *in vivo* (Figures 2 and 3), these dimers form independently of DNA binding, confirming the DNase experiments above. Finally, we generated a new *CDC13* allele (*cdc13-ob3-13m*), in which we changed 13 a.a. that were previously identified as key residues for the proper DNA binding of the OB3 domain

(Figure 8A; (23)). The Cdc13-ob3-13m protein is expressed in cells (Figure 7C), does not complement the *cdc13-1* mutation at 30°C (Figure 8B), and does not bind telomeric DNA as assessed by ChIP (Figure 8C). However, tagged versions of this protein still can be co-immunoprecipitated and it can also form a heterodimer when co-expressed with a wt version of Cdc13 (Figure 7C right panels and Supplementary Figure S6E far right). We therefore conclude that homodimer formation is independent of DNA binding. This result allowed us to test whether DNA binding *per se* was required for nuclear retention of the Cdc13 protein, given that the Cdc13-ob3Δ version lost both, dimerization and nuclear retention. Immunofluorescence of Myc-tagged Cdc13-ob3-13m on cycling adapted *cdc13Δ* cells showed a diffuse signal localized in both nucleus and cytoplasm, essentially an indistinguishable phenotype as obtained with the Cdc13-ob3Δ protein (Figure 8D; Supplementary Figure S5D). This result suggests that it is Cdc13 binding to telomeric G-strand DNA that retains it in the nucleus and prevents its export to the cytoplasm.

DISCUSSION

The linearity of eukaryotic chromosomes requires specialized mechanisms to keep their ends stable (1–3). In mammals, a highly ordered six-member complex called shelterin is at the center for this function. In addition, during replication, the heterotrimeric hCtc1/hStn1/hTen1 complex (hCST) participates in limiting telomerase mediated G-strand extension as well as initiating lagging C-strand synthesis (13,42). However, it is equally important that these normal telomeric capping mechanisms not be active on chromosomal ends occurring elsewhere in the genome after accidental DNA breaks.

In budding yeast, the trimeric Cdc13/Stn1/Ten (CST) complex is the key coordinating unit for telomeric sequence addition by telomerase and capping (1). CST has noted similarities with the trimeric ssDNA binding complex RPA and some of its functions may include those of a telomere specific RPA (22). Of the three CST proteins, Cdc13 is the one with high-affinity G-rich ssDNA binding and all telomeric functions depend on this capacity. Previous analyses of the full length Cdc13 protein or isolated fragments thereof have proposed an overall modular structure with four OB-fold domains and one recruitment domain between OB1 and OB2. Here we analyzed individual deletions of each of those domains and assessed the functions of the remaining protein in cells that harbor a *ts* allele of the gene (*CDC13-1*) or in cells that have adapted to grow without Cdc13 (40,41).

Our immunolocalization studies showed deletion of all of OB2 (Δ290–493) causes a striking exclusive cytoplasmic localization (Figure 3). Predictive algorithms suggested that Cdc13 has a classical nuclear localization signal (cNLS) between a.a. 325 and 350 (Figure 3), a region previously ascribed as the N-terminus of OB2 (Figures 1 and 3B). Moreover, the addition of a classical SV40-derived NLS in place of this deletion corrects this mislocalization (Figure 4A), suppresses the thermo-sensitivity of the *cdc13-1* allele at 30°C (Figure 4B–D) and, if expressed from a high copy plasmid, is sufficient to confer cellular viability on its own (Figure 4E). Furthermore, a deletion of only amino acids 329–

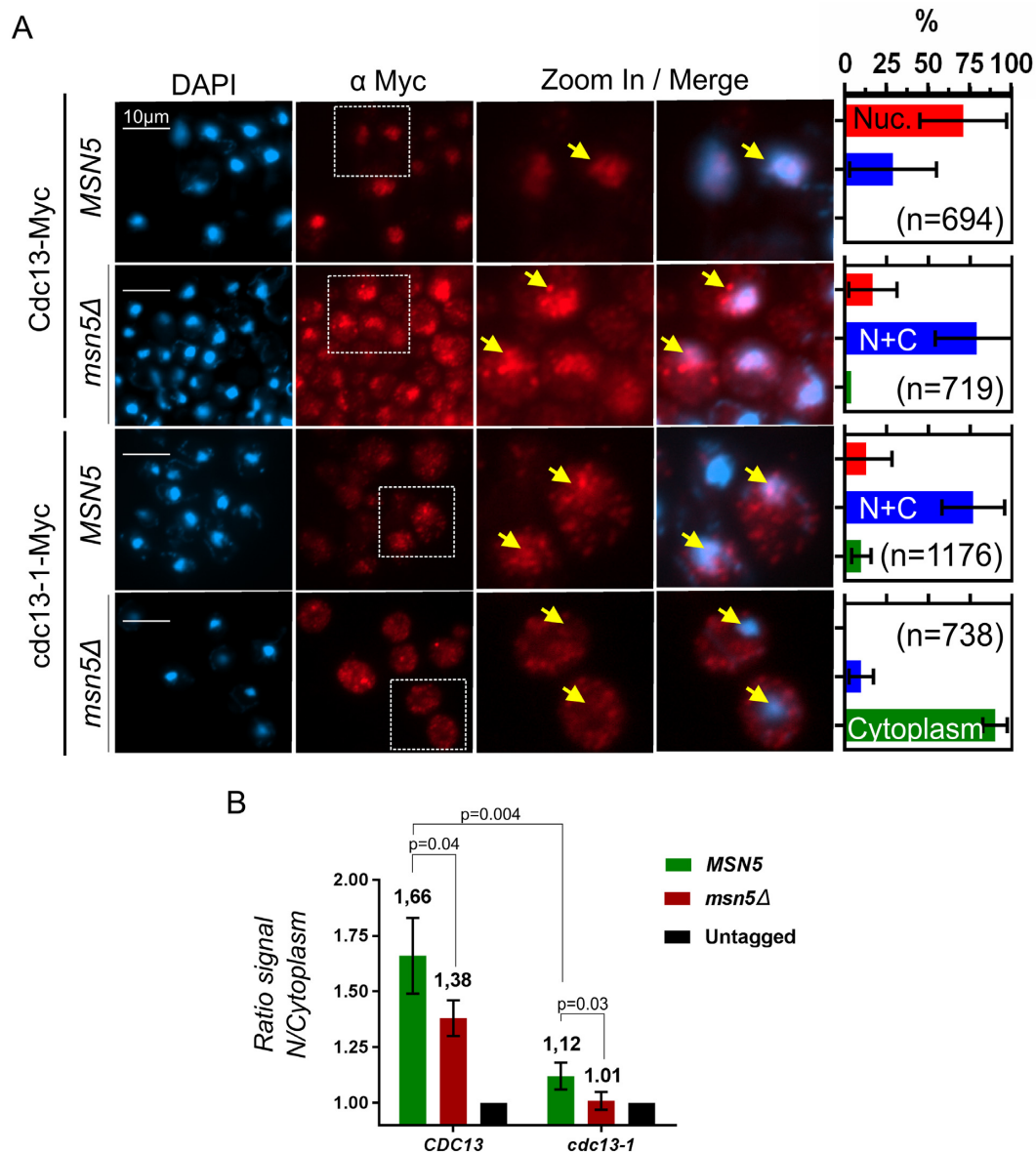


Figure 6. Loss of nuclear signal for Cdc13 in *msn5*Δ cells. (A) Subcellular localization of Myc-tagged wt Cdc13 or Cdc13-1 was assessed in *MSN5* or *msn5*Δ cells as indicated. All experiments were performed at 23°C and analyzed as above. (B) Quantification of the nuclear vs. cytoplasmic signal obtained with the anti-Myc antibody in the indicated strains and conditions as in (A). Untagged proteins are set as 1. Calculated Mean value is indicated on the top of each bar and error bars represent ± SEM. Indicated *P*-values (*p*) are provided by *t*-test between the two defined conditions.

368 also resulted in a non-functional Cdc13 (Supplementary Figure S4) and cytoplasmic localization (Figure 5A, bottom), suggesting that indeed, the essential function of the OB2 domain lies in mediating efficient import of Cdc13 into the nucleus and that this function is associated with the region 325–350 of OB2. Deleting the karyopherin Msn5 (Kap142) causes a significant shift of Cdc13 localization to the cytoplasm and an enhancement of the mislocalization of the Cdc13–1 protein, a phenotype that was also reported for the Rfa1 and Rfa2 proteins of RPA in *msn5*Δ cells (53). In addition, Msn5 had already been described as a phenotypic enhancer for the *cdc13-1* allele (51). It is therefore reasonable to propose that nuclear import of Cdc13 is mediated by its NLS at a.a. 325–349 and that Msn5 contributes to

it. However, Msn5-mediated nuclear localization can only be part of the import mechanism, given that a deletion of *MSN5* is viable, yet nuclear localization of the Rfa1, Rfa2 and Cdc13 proteins is essential for their function. Currently, we do not know what other and redundant pathways ensure import in the absence of Msn5. Specifically for the Cdc13–1 protein, we cannot completely exclude an additional contribution of the San1-mediated protein degradation pathway to the observed phenotypes (51,54).

Our co-immunoprecipitation approach confirmed previous suggestions of an area in OB1 (a.a. 80–120) that is important for dimerization of the protein (Figure 7C). In addition, the detailed analysis of the newly constructed alleles (OB2Δ, OB3-13m) shows that Cdc13 dimerization oc-

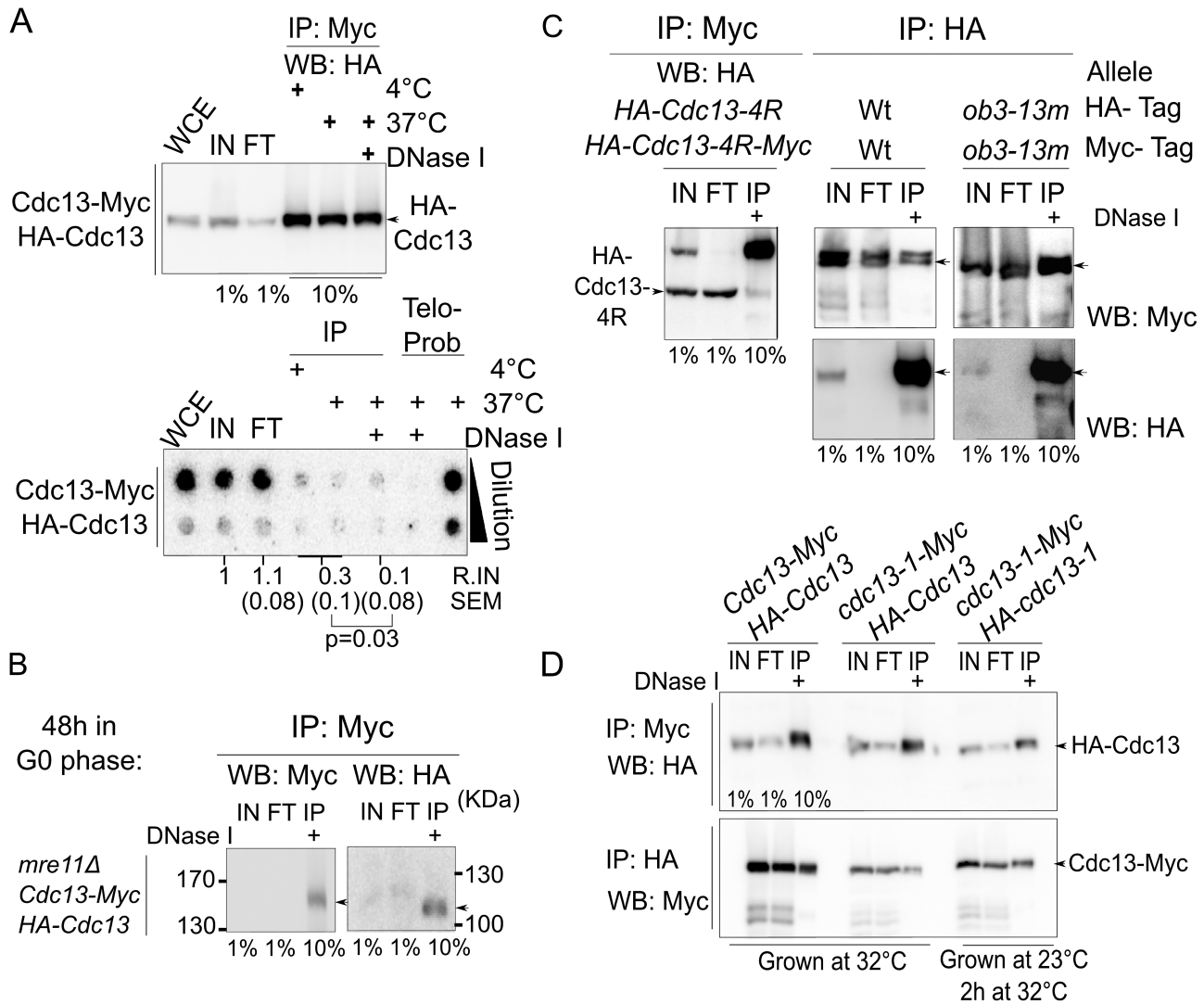


Figure 7. Co-immunoprecipitation of differentially tagged Cdc13 proteins. (A) Upper panel: Western blot probed with anti-HA antibodies after immunoprecipitation of protein extracts with anti-Myc. WCE: whole cell extract (before IP); IN: Input after centrifugal clearing of the WCE; FT: Flow through. Temperatures of the experiments and 1h DNase I treatment at 37°C before IP are indicated on right. Percentage indicates volume loaded relative to the Input. Lower panel: dot blot analysis after DNA extraction obtained from the same samples shown in the upper panel, and hybridized with telomeric probe PCT300. An aliquot of unlabeled PCT300 is used as a hybridization control (Telo-Prob). Signals of dots were quantified relative to the Input (R.IN) and the SEM from three independent experiments are indicated. Note the loss of DNA signal in the IPs with DNase treatment. (B) Co-immunoprecipitation of the two differentially tagged Cdc13 proteins in an *mre11Δ* background after extended G0 cell arrest. IPs are treated for 1h with DNase I at 37°C as indicated. (C) Left: Loss of Cdc13 dimerization if one of the proteins contains the 4R mutations. Western blot of precipitates from IP experiments derived from strains expressing the indicated proteins. Right: Co-immunoprecipitation of the Cdc13-ob3-13m dimer (see also reverse experiment in Supplementary Figure S4E). (D) Co-immunoprecipitation experiment of two *cdc13-1* proteins tagged respectively with 13-Myc and 3xHA, and co-expressed from two independent plasmids. Strains are grown as indicated.

curs constitutively and that dimerization is not dependent on DNA binding (Figures 7, 8 and Supplementary Figure S6). These data therefore predict that the stoichiometry of the CST complex is not a simple 1:1:1 ratio, as would be expected from a strict RPA parallelism. Rather, the results strongly suggest that Cdc13 functions as a dimer for the telomerase recruitment function, perhaps independently from the Stn1-Ten1 proteins (35). There is evidence for such an altered stoichiometry with at least two Cdc13 molecules in the CST complex also for the *C. glabrata* CST (30). While the data suggest a contribution to dimerization by the OB3 domain (Supplementary Figure S6E), it is

possible that this particular protein is misfolded and cannot assume any function anymore. Nevertheless, the Cdc13-OB2Δ and the Cdc13-1 proteins, which both have a wt OB1 and OB3 do dimerize (Figure 7 and Supplementary Figure S6E) and both mislocalize to the cytoplasm (Figures 3 and 5). Therefore, dimerization occurs in the cytoplasm, presumably before nuclear import for the wt protein and is independent from DNA binding (Figures 3, 7 and 8). We speculate that dimerization of Cdc13 may be required to render the protein stable. Consistent with this possibility, mutations that delete the dimerization area in OB1 (Cdc13-

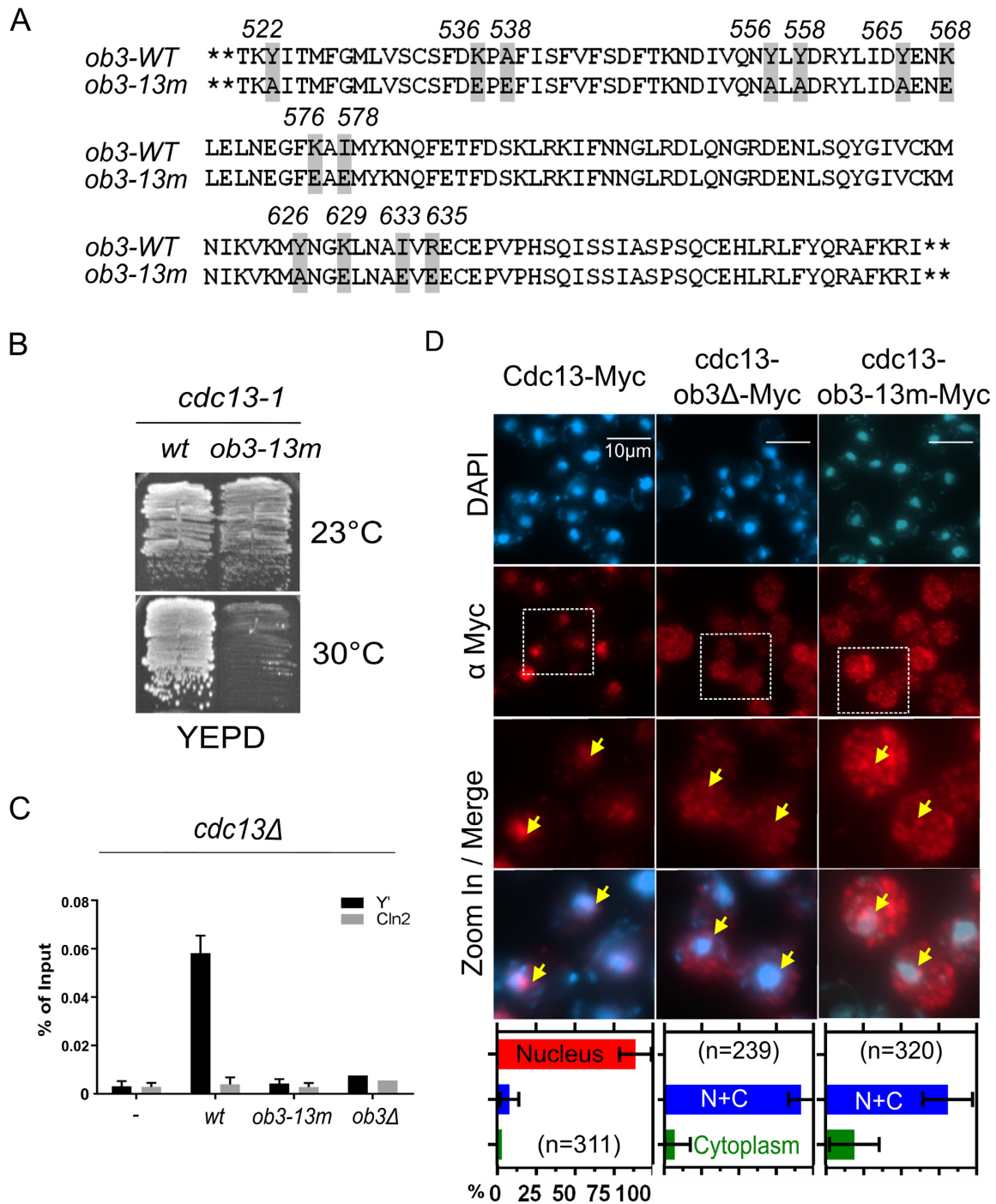


Figure 8. DNA association is not required for dimerization of Cdc13. (A) Sequence and position of the 13 a.a. residues changed in the DNA-binding defective *cdc13-ob3-13m* allele as compared to the wild type sequence. The modified residues are highlighted and the amino acid position within the protein is indicated on top. (B) Complementation test of the DNA-binding-defective *cdc13-ob3-13m* allele in the *cdc13-1* strain at restrictive temperature. (C) Chromatin-IP experiment on the Cdc13-*ob3-13m* versus the Cdc13-*ob3Δ* variant expressed in the adapted *cdc13Δ* strains. (D) Immunofluorescence on cell of an adapted *cdc13Δ* strain expressing the Cdc13-*ob3Δ* or the Cdc13-*ob3-13m* protein. Analyses of the images as in Figure 3.

ob1 Δ , Figure 1) cause a destabilization of Cdc13 (Figure 1C, Supplementary Figure S1D).

Interestingly, an inspection of the crystallized OB2 domain shows that in fact there is no structural information on the newly discovered NLS region (a.a. 325–350) in OB2. The first α -helical segment that is recognizable in the structure for OB2 starts at a.a. 348 and the classical OB fold is contained between a.a. 355 and 475 (29). Therefore, we propose that there is a new separate functional element, comprising the cNLS (325–350) between the RD domain and the actual OB2. This NLS domain mediates nuclear import and is essential for the *in vivo* function of Cdc13. Further, our data are consistent with the idea that the *cdc13-1* (P371S) mutation interferes with NLS function. In the absence of structural information of the whole protein, one can only speculate on the changes that occur in the Cdc13–1 protein. We suppose a temperature-aggravated structural change of this area of the protein may cause an occlusion of the nearby NLS, leading to an absence of the protein from the nucleus and hence the observed phenotypes. Our results also show that DNA binding is required for nuclear retention of Cdc13 (Figures 3 and 8). Hence in a DNA binding mutant (the *cdc13-ob3-13m* allele), the protein displays a non-discriminate nuclear and cytoplasmic distribution. We interpret these data to mean that any Cdc13 protein not bound to DNA may be released to the cytoplasm, followed by cycles of import and export. For the wt protein, this would help prevent association of free Cdc13 to non-telomeric sites where it could stimulate inappropriate new telomere synthesis. Such non-telomeric DNA association is possible and Cdc13 phosphorylation has been proposed as one mechanism to limit off-target telomere formation (55). Our data here suggest that Cdc13 release to the cytoplasm has a major contribution to that genome stabilizing mechanism.

Our conclusions neatly rationalize and explain a plethora of data in the relatively extensive literature that uses *cdc13-1* as a DNA damage and checkpoint inducing system. In addition, mutations with similar cytoplasmic mislocalization have recently been described for the hCTC1 protein that is part of the human CST (42). The alleles causing cytoplasmic localization phenotype in human cells are directly associated with the rare, but severe Coats Plus disease, a syndrome that now is part of telomere associated diseases (56–58). Strikingly, disease-causing CTC1 alleles as well as the *cdc13-1* allele cause cellular pathologies that are related to telomere dysfunction, but not necessarily with short telomeres (42). In addition, in both systems accumulation of single-stranded DNA appears to be a key characteristic associated with these alleles. Finally, certain hCTC1 alleles cause a loss of telomerase-mediated lengthening control, a feature that is also associated with *cdc13-1* at semi permissive temperature or after the loss of the OB4 domain ((35); Figures 1 and 4). Therefore, given the overall structural and functional similarities between the budding yeast Cdc13 and the human CTC1, we propose that the yeast *cdc13-1* allele could be used as a model system for investigations on treating the human disease caused by hCTC1 mutations. The results presented here would suggest that approaches stimulating nuclear import could become promising avenues in this regard.

SUPPLEMENTARY DATA

Supplementary Data are available at NAR Online.

ACKNOWLEDGEMENTS

We thank V. Lundblad for sharing a number of constructs and plasmids. M. Catala and E. Bajon helped with the initial microscopy techniques and the members of the Wellinger lab for stimulating discussions.

FUNDING

Canadian Institutes of Health Research [MOP 110982]; Canadian Research Chair in Telomere Biology; Sherbrooke RNA Group. Funding for open access charge: Canadian Institutes for Health Research.

Conflict of interest statement. None declared.

REFERENCES

- Wellinger, R.J. and Zakian, V.A. (2012) Everything you ever wanted to know about *Saccharomyces cerevisiae* telomeres: beginning to end. *Genetics*, **191**, 1073–1105.
- Palm, W. and de Lange, T. (2008) How shelterin protects mammalian telomeres. *Annu. Rev. Genet.*, **42**, 301–334.
- Schmutz, I. and de Lange, T. (2016) Shelterin. *Curr. Biol.*, **26**, R397–R399.
- Wellinger, R.J. (2014) In the end, what's the problem? *Mol. Cell*, **53**, 855–856.
- Wu, R.A., Upton, H.E., Vogan, J.M. and Collins, K. (2017) Telomerase mechanism of telomere synthesis. *Annu. Rev. Biochem.*, **86**, 439–460.
- Greider, C.W. and Blackburn, E.H. (1987) The telomere terminal transferase of *Tetrahymena* is a ribonucleoprotein enzyme with two kinds of primer specificity. *Cell*, **51**, 887–898.
- Grandin, N., Damon, C. and Charbonneau, M. (2001) Ten1 functions in telomere end protection and length regulation in association with Stn1 and Cdc13. *EMBO J.*, **20**, 1173–1183.
- Grandin, N., Reed, S.I. and Charbonneau, M. (1997) Stn1, a new *Saccharomyces cerevisiae* protein, is implicated in telomere size regulation in association with Cdc13. *Genes Dev.*, **11**, 512–527.
- Garvik, B., Carson, M. and Hartwell, L. (1995) Single-stranded DNA arising at telomeres in *cdc13* mutants may constitute a specific signal for the RAD9 checkpoint. *Mol. Cell Biol.*, **15**, 6128–6138.
- Takikawa, M., Tarumoto, Y. and Ishikawa, F. (2017) Fission yeast Stn1 is crucial for semi-conservative replication at telomeres and subtelomeres. *Nucleic Acids Res.*, **45**, 1255–1269.
- Lee, J.R., Xie, X., Yang, K., Zhang, J., Lee, S.Y. and Shippen, D.E. (2016) Dynamic interactions of Arabidopsis TEN1: stabilizing telomeres in response to heat stress. *Plant Cell*, **28**, 2212–2224.
- Chastain, M., Zhou, Q., Shiva, O., Whitmore, L., Jia, P., Dai, X., Huang, C., Fadri-Moskwick, M., Ye, P. and Chai, W. (2016) Human CST facilitates genome-wide RAD51 recruitment to GC-rich repetitive sequences in response to replication stress. *Cell Rep.*, **16**, 1300–1314.
- Chen, L.Y. and Lingner, J. (2013) CST for the grand finale of telomere replication. *Nucleus*, **4**, 277–282.
- Wellinger, R.J. (2009) The CST complex and telomere maintenance: the exception becomes the rule. *Mol. Cell*, **36**, 168–169.
- Surovtseva, Y.V., Churikov, D., Boltz, K.A., Song, X., Lamb, J.C., Warrington, R., Leehy, K., Heacock, M., Price, C.M. and Shippen, D.E. (2009) Conserved telomere maintenance component 1 interacts with STN1 and maintains chromosome ends in higher eukaryotes. *Mol. Cell*, **36**, 207–218.
- Miyake, Y., Nakamura, M., Nabetani, A., Shimamura, S., Tamura, M., Yonehara, S., Saito, M. and Ishikawa, F. (2009) RPA-like mammalian Ctc1-Stn1-Ten1 complex binds to single-stranded DNA and protects telomeres independently of the Pot1 pathway. *Mol. Cell*, **36**, 193–206.
- Cicconi, A., Micheli, E., Verni, F., Jackson, A., Gradilla, A.C., Cipressa, F., Raimondo, D., Bosso, G., Wakefield, J.G., Ciapponi, L. *et al.* (2017) The *Drosophila* telomere-capping protein Verrocchio

- binds single-stranded DNA and protects telomeres from DNA damage response. *Nucleic Acids Res.*, **45**, 3068–3085.
18. Zhang, Y., Zhang, L., Tang, X., Bhardwaj, S.R., Ji, J. and Rong, Y.S. (2016) MTV, an ssDNA protecting complex essential for transposon-based telomere maintenance in *Drosophila*. *PLoS Genet.*, **12**, e1006435.
 19. Simon, A.J., Lev, A., Zhang, Y., Weiss, B., Rylova, A., Eyal, E., Kol, N., Barel, O., Cesarkas, K., Soudack, M. *et al.* (2016) Mutations in STN1 cause Coats plus syndrome and are associated with genomic and telomere defects. *J. Exp. Med.*, **213**, 1429–1440.
 20. Rice, C. and Skordalakes, E. (2016) Structure and function of the telomeric CST complex. *Comput. Struct. Biotechnol. J.*, **14**, 161–167.
 21. Sun, J., Yang, Y., Wan, K., Mao, N., Yu, T.Y., Lin, Y.C., DeZwaan, D.C., Freeman, B.C., Lin, J.J., Lue, N.F. *et al.* (2011) Structural bases of dimerization of yeast telomere protein Cdc13 and its interaction with the catalytic subunit of DNA polymerase alpha. *Cell Res.*, **21**, 258–274.
 22. Gao, H., Cervantes, R.B., Mandell, E.K., Otero, J.H. and Lundblad, V. (2007) RPA-like proteins mediate yeast telomere function. *Nat. Struct. Mol. Biol.*, **14**, 208–214.
 23. Mitton-Fry, R.M., Anderson, E.M., Hughes, T.R., Lundblad, V. and Wuttke, D.S. (2002) Conserved structure for single-stranded telomeric DNA recognition. *Science*, **296**, 145–147.
 24. Hughes, T.R., Weilbaecher, R.G., Walterscheid, M. and Lundblad, V. (2000) Identification of the single-strand telomeric DNA binding domain of the *Saccharomyces cerevisiae* Cdc13 protein. *Proc. Natl. Acad. Sci. U.S.A.*, **97**, 6457–6462.
 25. Nugent, C.I., Hughes, T.R., Lue, N.F. and Lundblad, V. (1996) Cdc13p: a single-strand telomeric DNA-binding protein with a dual role in yeast telomere maintenance. *Science*, **274**, 249–252.
 26. Lin, J.J. and Zakian, V.A. (1996) The *Saccharomyces* CDC13 protein is a single-strand TG1-3 telomeric DNA-binding protein in vitro that affects telomere behavior in vivo. *Proc. Natl. Acad. Sci. U.S.A.*, **93**, 13760–13765.
 27. Wang, M.J., Lin, Y.C., Pang, T.L., Lee, J.M., Chou, C.C. and Lin, J.J. (2000) Telomere-binding and Stn1p-interacting activities are required for the essential function of *Saccharomyces cerevisiae* Cdc13p. *Nucleic Acids Res.*, **28**, 4733–4741.
 28. Lewis, K.A., Pfaff, D.A., Earley, J.N., Altschuler, S.E. and Wuttke, D.S. (2014) The tenacious recognition of yeast telomere sequence by Cdc13 is fully exerted by a single OB-fold domain. *Nucleic Acids Res.*, **42**, 475–484.
 29. Mason, M., Wanat, J.J., Harper, S., Schultz, D.C., Speicher, D.W., Johnson, F.B. and Skordalakes, E. (2013) Cdc13 OB2 dimerization required for productive Stn1 binding and efficient telomere maintenance. *Structure*, **21**, 109–120.
 30. Lue, N.F., Zhou, R., Chico, L., Mao, N., Steinberg-Neifach, O. and Ha, T. (2013) The telomere capping complex CST has an unusual stoichiometry, makes multipartite interaction with G-Tails, and unfolds higher-order G-tail structures. *PLoS Genet.*, **9**, e1003145.
 31. Mitchell, M.T., Smith, J.S., Mason, M., Harper, S., Speicher, D.W., Johnson, F.B. and Skordalakes, E. (2010) Cdc13 N-terminal dimerization, DNA binding, and telomere length regulation. *Mol. Cell Biol.*, **30**, 5325–5334.
 32. Mitton-Fry, R.M., Anderson, E.M., Theobald, D.L., Glustrom, L.W. and Wuttke, D.S. (2004) Structural basis for telomeric single-stranded DNA recognition by yeast Cdc13. *J. Mol. Biol.*, **338**, 241–255.
 33. Hsu, C.L., Chen, Y.S., Tsai, S.Y., Tu, P.J., Wang, M.J. and Lin, J.J. (2004) Interaction of *Saccharomyces* Cdc13p with Pol1p, Imp4p, Sir4p and Zds2p is involved in telomere replication, telomere maintenance and cell growth control. *Nucleic Acids Res.*, **32**, 511–521.
 34. Qi, H. and Zakian, V.A. (2000) The *Saccharomyces* telomere-binding protein Cdc13p interacts with both the catalytic subunit of DNA polymerase alpha and the telomerase-associated est1 protein. *Genes Dev.*, **14**, 1777–1788.
 35. Chandra, A., Hughes, T.R., Nugent, C.I. and Lundblad, V. (2001) Cdc13 both positively and negatively regulates telomere replication. *Genes Dev.*, **15**, 404–414.
 36. Pennock, E., Buckley, K. and Lundblad, V. (2001) Cdc13 delivers separate complexes to the telomere for end protection and replication. *Cell*, **104**, 387–396.
 37. Lendvay, T.S., Morris, D.K., Sah, J., Balasubramanian, B. and Lundblad, V. (1996) Senescence mutants of *Saccharomyces cerevisiae* with a defect in telomere replication identify three additional EST genes. *Genetics*, **144**, 1399–1412.
 38. Singer, M.S. and Gottschling, D.E. (1994) TLC1: template RNA component of *Saccharomyces cerevisiae* telomerase. *Science*, **266**, 404–409.
 39. Hang, L.E., Liu, X., Cheung, I., Yang, Y. and Zhao, X. (2011) SUMOylation regulates telomere length homeostasis by targeting Cdc13. *Nat. Struct. Mol. Biol.*, **18**, 920–926.
 40. Mersaoui, S.Y., Gravel, S., Karpov, V. and Wellinger, R.J. (2015) DNA damage checkpoint adaptation genes are required for division of cells harbouring eroded telomeres. *Microb. Cell*, **2**, 394–405.
 41. Larrivee, M. and Wellinger, R.J. (2006) Telomerase- and capping-independent yeast survivors with alternate telomere states. *Nat. Cell Biol.*, **8**, 741–747.
 42. Chen, L.Y., Majerska, J. and Lingner, J. (2013) Molecular basis of telomere syndrome caused by CTC1 mutations. *Genes Dev.*, **27**, 2099–2108.
 43. Wellinger, R.J., Wolf, A.J. and Zakian, V.A. (1993) Origin activation and formation of single-strand TG1-3 tails occur sequentially in late S phase on a yeast linear plasmid. *Mol. Cell Biol.*, **13**, 4057–4065.
 44. Dionne, I. and Wellinger, R.J. (1996) Cell cycle-regulated generation of single-stranded G-rich DNA in the absence of telomerase. *Proc. Natl. Acad. Sci. U.S.A.*, **93**, 13902–13907.
 45. Fisher, T.S., Taggart, A.K.P. and Zakian, V.A. (2004) Cell cycle-dependent regulation of yeast telomerase by Ku. *Nat. Struct. Mol. Biol.*, **11**, 1198–1205.
 46. Taggart, A.K., Teng, S.C. and Zakian, V.A. (2002) Est1p as a cell cycle-regulated activator of telomere-bound telomerase. *Science*, **297**, 1023–1026.
 47. Bajon, E., Laterreur, N. and Wellinger, R.J. (2015) A single templating RNA in yeast telomerase. *Cell Rep.*, **12**, 441–448.
 48. Teng, S.C. and Zakian, V.A. (1999) Telomere-telomere recombination is an efficient bypass pathway for telomere maintenance in *Saccharomyces cerevisiae*. *Mol. Cell Biol.*, **19**, 8083–8093.
 49. Vodenicharov, M.D., Laterreur, N. and Wellinger, R.J. (2010) Telomere capping in non-dividing yeast cells requires Yku and Rap1. *EMBO J.*, **29**, 3007–3019.
 50. Kosugi, S., Hasebe, M., Tomita, M. and Yanagawa, H. (2009) Systematic identification of cell cycle-dependent yeast nucleocytoplasmic shuttling proteins by prediction of composite motifs. *Proc. Natl. Acad. Sci. U.S.A.*, **106**, 10171–10176.
 51. Addinall, S.G., Holstein, E.M., Lawless, C., Yu, M., Chapman, K., Banks, A.P., Ngo, H.P., Maringele, L., Taschuk, M., Young, A. *et al.* (2011) Quantitative fitness analysis shows that NMD proteins and many other protein complexes suppress or enhance distinct telomere cap defects. *PLoS Genet.*, **7**, e1001362.
 52. Larrivee, M., LeBel, C. and Wellinger, R.J. (2004) The generation of proper constitutive G-tails on yeast telomeres is dependent on the MRX complex. *Genes Dev.*, **18**, 1391–1396.
 53. Yoshida, K. and Blobel, G. (2001) The karyopherin Kap142p/Msn5p mediates nuclear import and nuclear export of different cargo proteins. *J. Cell Biol.*, **152**, 729–740.
 54. Gardner, R.G., Nelson, Z.W. and Gottschling, D.E. (2005) Degradation-mediated protein quality control in the nucleus. *Cell*, **120**, 803–815.
 55. Zhang, W. and Durocher, D. (2010) De novo telomere formation is suppressed by the Mec1-dependent inhibition of Cdc13 accumulation at DNA breaks. *Genes Dev.*, **24**, 502–515.
 56. Polvi, A., Linnankivi, T., Kivela, T., Herva, R., Keating, J.P., Makitie, O., Pareyson, D., Vainionpaa, L., Lahtinen, J., Hovatta, I. *et al.* (2012) Mutations in CTC1, encoding the CTS telomere maintenance complex component 1, cause cerebrotendinous microangiopathy with calcifications and cysts. *Am. J. Hum. Genet.*, **90**, 540–549.
 57. Keller, R.B., Gagne, K.E., Usmani, G.N., Asdourian, G.K., Williams, D.A., Hofmann, I. and Agarwal, S. (2012) CTC1 Mutations in a patient with dyskeratosis congenita. *Pediatr. Blood Cancer*, **59**, 311–314.
 58. Anderson, B.H., Kasher, P.R., Mayer, J., Szykiewicz, M., Jenkinson, E.M., Bhaskar, S.S., Urquhart, J.E., Daly, S.B., Dickerson, J.E., O'Sullivan, J. *et al.* (2012) Mutations in CTC1, encoding conserved telomere maintenance component 1, cause Coats plus. *Nat. Genet.*, **44**, 338–342.